Journal of Electronics and Electrical Engineering
https://ojs.wiserpub.com/index.php/JEEE

Research Article

A Novel ANFIS Controller for LFC in RES Integrated Three-Area Power System

Yaw Opoku Mensah Sekyere*, Francis Boafo Effah, Philip Yaw Okyere

Electrical Engineering Department, Kwame Nkrumah University of Science and Technology, Kumasi, Ghana
E-mail: Yawsekyere@gmail.com

Received: 7 May 2024; **Revised:** 10 July 2024; **Accepted:** 30 July 2024

Abstract: This paper presents a novel Adaptive Neuro-Fuzzy Inference System (ANFIS) model for Load Frequency Control (LFC) with an expanded input configuration, incorporating the integral of the area control error (ACE) alongside the traditional ACE and its derivative. This additional input captures historical ACE trends, enhancing the ANFIS control performance. The ANFIS training dataset, comprising ACE error, its derivative, and integral, is generated using a PID controller tuned by a variant of Particle Swarm Optimization (PSO) algorithm called an Adaptive Dynamic Inertia Weight Acceleration Coefficient (ADIWACO). Its evaluation on a three-area power system with renewable energy sources (RES) includes comparative analysis with PID, traditional 2-input ANFIS, Fuzzy Logic, and Artificial Neural Network (ANN) controllers. Simulation results demonstrate the superior performance of the proposed 3-input ANFIS controller in terms of performance metrics, consisting of overshoot, undershoot, settling time, steady-state error, and Integral Time Absolute Error (ITAE). Notably, the proposed ANFIS model shows a significant 75.89% improvement in ITAE value over the traditional 2-input ANFIS when communication delays and governor dead band constraints are considered, underscoring the significant impact of the additional input. System parameters variation of ±25%, further confirms the controller's robustness to uncertain model parameters. This study contributes to advancing real-world application of ANFIS controllers for LFC in interconnected power systems integrated with the two most widely developed renewable resources, namely solar and wind power plants.

Keywords: Load Frequency Control (LFC), Adaptive Neuro-Fuzzy Inference System (ANFIS), Particle Swarm Optimization (PSO), ADIWACO

Abbreviation

ACE	Area Control Error
ACO	Ant Colony Optimization
ADIWACO	Adaptive Dynamic Inertia Weight Acceleration Coefficient
ANFIS	Adaptive Neuro Fuzzy Inference System
ANN	Artificial Neural Network

DOI: https://doi.org/10.37256/jeee.3220244886

CTD	Communication Time Delay
GDB	Governor Dead Band
GWO	Grey Wolf Optimization
ICA	Imperialist Competitive Algorithm
ITAE	Integral Time Absolute Error
LFC	Load Frequency Control
PID	Proportional Integral Derivative
PSO	Particle Swarm Optimization
RES	Renewable Energy Sources
TLBO	Teaching and Learning Based Optimization

1. Introduction

The evolving landscape of power systems is witnessing a significant paradigm shift driven by the increasing penetration of renewable energy sources (RES) [1, 2]. This transition introduces new dynamics and challenges, particularly in load frequency control (LFC), which is required to maintain the stability and reliability of power systems [3]. Traditionally, LFC has been primarily designed to manage load-generation balance in response to fluctuations to ensure that the frequency of the power system remains within acceptable limits. With the growing penetration of solar and wind power plants, characterized by inherent intermittency and unpredictability, the traditional control strategies may struggle to address load and generation imbalances [4, 5, 6, 7, 8]. Consequently, innovative control strategies that can adapt to these changing conditions have become necessary [3, 4, 5, 6]. A review of pertinent literature reveals key trends and advances in LFC methodologies. Classical LFC approaches often rely on proportional-integral (PI) [8, 9, 10, 11, 12] and proportional-integral-derivative (PID) controllers [3, 13] control system frequency in response to load and generation imbalances. While these traditional controllers have demonstrated effectiveness in conventional power systems, their adaptability to the variability and intermittency introduced by RES remains a subject of investigation [14].

Recent studies have explored the enhancements of classical PID controllers and innovative fixed gain controller structures such as cascaded PI-PD [15], PD-PI [16], TID-PID [17], PD-PID plus double derivative filters [18] through metaheuristic tuning algorithms for LFC in power systems with RES. Some of the most widely used metaheuristic algorithms in the literature for optimal tuning of fixed gain controller structures are the Particle Swarm Optimization (PSO) [3, 19, 20], Grey Wolf Optimization (GWO) [11], Ant Colony Optimization (ACO) [21], Teaching Learning Based Optimization (TLBO) [17] and Imperialist Competitive Algorithm (ICA) [22, 23]. Intelligent controller-based strategies, such as Fuzzy Logic [24, 25], Artificial Neural Networks (ANNs) [26, 27, 28], and Reinforcement Learning-based strategies [29, 30, 31] have gained attention for their ability to adapt to nonlinear and time-varying systems. Fuzzy Logic controllers utilize linguistic rules to approximate complex relationships, while ANN leverages the learning capabilities of neural networks to adapt to system dynamics [32]. The integration of adaptive neuro-fuzzy inference systems (ANFIS) into LFC frameworks represents a notable trend in recent research. ANFIS merges the adaptive learning of ANN with the interpretability of fuzzy logic, offering a hybrid solution that captures both the precision of numerical methods and the interpretability of rule-based systems [32, 33, 34]. ANFIS controllers excel in capturing complex and non-linear relationships within power systems, making them well-suited for LFC [32, 35, 36]. By employing a hybrid structure that combines fuzzy inference rules with neural network training, ANFIS controllers can adapt to the dynamic nature of power systems, particularly in scenarios with RES integration [37]. A noteworthy example of ANFIS-based LFC proposed in the literature is the study conducted in [31] where the training data for ANFIS was obtained from a PID controller tuned by Honey Badger Algorithm (HBA). Several other examples of ANFIS-based LFC documented in [34, 35, 36, 37, 38] leveraged fuzzy logic controllers to generate the training dataset.

The existing ANFIS-based LFC strategies in interconnected power systems have several weaknesses. These include substantial computational demands associated with the parameter optimization process and generation of fuzzy rules based on the total number of membership functions [39, 40]. Though ANFIS controllers are designed to handle nonlinear systems, they may struggle with highly complex nonlinearities [39]. They may lack robustness, particularly in dealing with dynamic

load changes or generation disturbances [41]. Furthermore, the sensitivity of ANFIS performance to the quality of its training data introduces concerns about their reliability in real-world scenarios [42]. ANFIS controllers may also struggle with generalization outside of their training dataset, posing challenges in adapting to varying operating conditions [41]. These weaknesses call for more robust and adaptable control approaches. Existing methods for improving the performance of ANFIS controllers have primarily centred on the quality of the training data [32, 35, 36]. This study shifts the paradigm by introducing one more input signal in addition to using quality training dataset.

The existing ANFIS controllers for LFC in interconnected power systems integrated with RES have two input signals consisting of the ACE and the derivative of ACE. This paper introduces a novel ANFIS controller that adds the integral of ACE to the input signals to make them three. The integral of ACE signal captures the historical trends of ACE and its addition to the two traditional input signals improves the performance of the ANFIS controller. Additionally, the training dataset is generated by a PID controller tuned by a variant of PSO algorithm known as Adaptive Dynamic Inertia Weight Acceleration Coefficient Optimization (ADIWACO) [43]. The ADIWACO-tuned PID controller has proved to provide effective LFC in power systems with RES [2].

The ANFIS controller, proposed in this paper, is validated on an interconnected power system with three control areas integrated with RES. To confirm its efficacy in real-world scenarios, governor dead band and communication time delay are included in the model of the power system in one experimental scenario. The controller's robustness to uncertain model parameters is also verified using system parameter variation of ±25%.

1.1 *Contribution of the paper*

This makes the following significant contributions:

(i) It enhances the traditional ANFIS used for LFC by incorporating the integral of the Area Control Error (ACE) into the traditional inputs, which are ACE and its derivative.

(ii) It generates high-quality training data by employing an ADIWACO-tuned Proportional-Integral-Derivative (PID) controller.

1.2 *Paper organization*

The subsequent sections of the paper are organized as follows: Section 2 presents the introduces the test system used for evaluating the proposed ANFIS controller, outlines the theoretical framework for ANFIS controllers and details the proposed ANFIS controller and its training algorithm. Section 3 presents the results and discussion, and Section 4 concludes the paper and discusses future research directions.

2. IEEE 39-bus test system

The IEEE 39-bus system has been modified as a case study to analyze load frequency control for a RES-integrated multi-area power system. The IEEE 39-bus system, comprising 10 conventional thermal plant generators, 39 buses, and 46 branches, has been modified by dividing it into three control areas and integrating wind and solar generation units at buses 7 and 8, respectively as depicted in Figure 1. The three control areas, with a capacity ratio of 2:5:8, are simplified in Figure 2 by grouping all coherent generators in each area into a single thermal reheat plant. It is assumed that all conventional power plants participate in the load frequency control. Each plant includes a governor, turbine, reheater, primary droop control, and supplementary LFC control to manage system frequency and tie-line power flows. The integration of RES within control Area 1 reflects the modern trend of incorporating renewable energy into traditional power systems. This model has been widely used in the literature for load frequency control studies [9, 13, 17, 22, 24, 44, 45, 46, 47, 48]. The transfer functions for wind turbine plant, $G(s)_W$ and solar PV plant, $G(s)_{PV}$, which are not detailed in Figure 2 are given by (1) and (2) [9]:

$$G(s)_W = \frac{K_W}{1+sT_W} \tag{1}$$

$$G(s)_{PV} = \frac{K_{PV}}{1+sT_{PV}} \tag{2}$$

where K_W is the gain of the wind turbine plant and K_{PV} is that of the solar PV. The parameters T_W and T_{PV} are their respective time constants. The transfer functions of the other components are detailed in Figure 2. The specifications of the test system and the values of the various constants used for the study are provided in the Appendix.

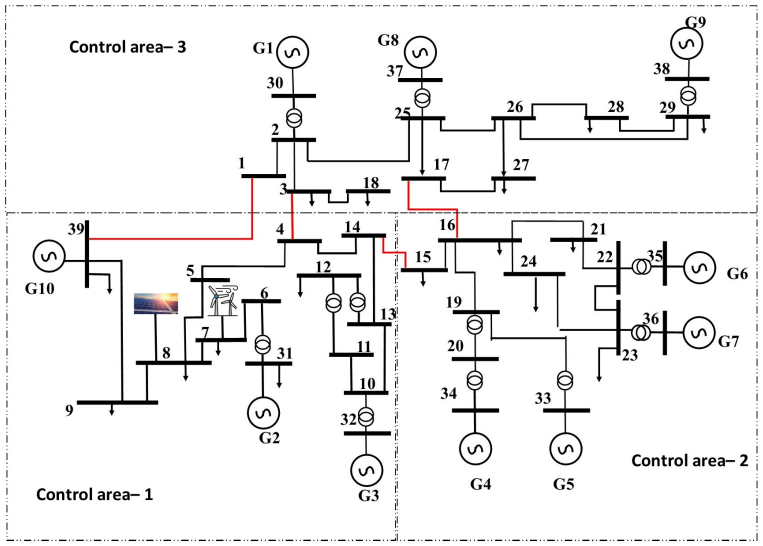

Figure 1. IEEE 39-bus Test System

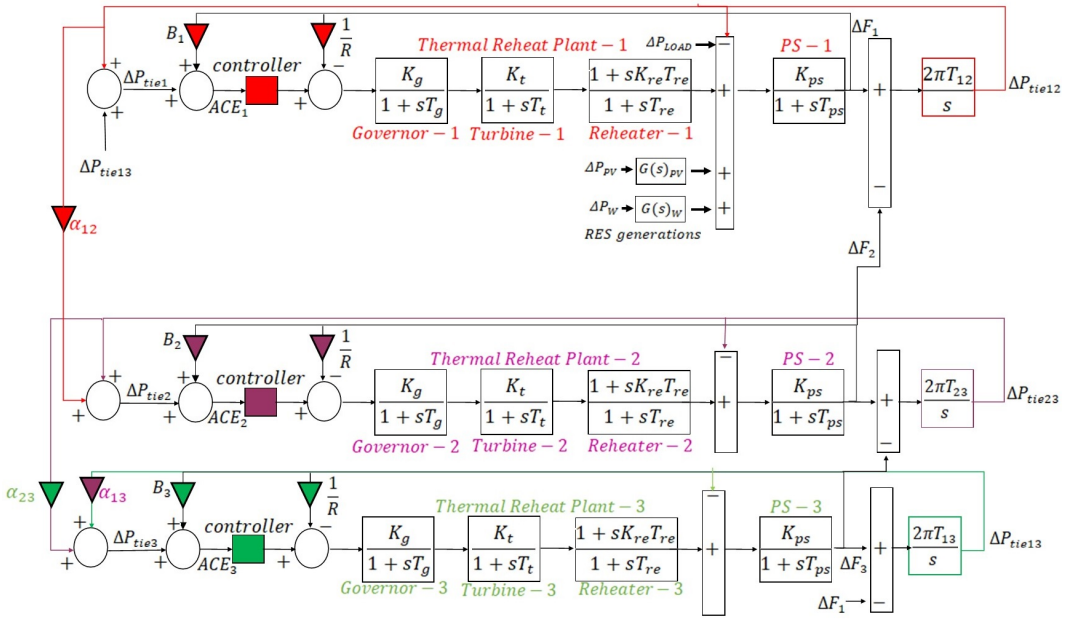

Figure 2. Simplified Test System

2.1 *ANFIS controller*

The ANFIS controller is a sophisticated multilayered controller having fuzzy logic and neural network components [37]. The main advantage of ANFIS over the Fuzzy Inference System (FIS) is that it replaces the manually set rules of the FIS component and the fine tuning of its parameters by a knowledge-based ANN [36]. The ANN, based on dataset that are used to train it, comes up with appropriate rules for the control process. During the process of making the rules, parameters of membership functions can also be dynamically adjusted for optimal control performance [32]. The general architecture of ANFIS is shown in Figure 3. It has two inputs x and y and a single output f. The layers one and four host adaptive nodes whereas layers two, three and five consist of fixed nodes with no adjustable parameters.

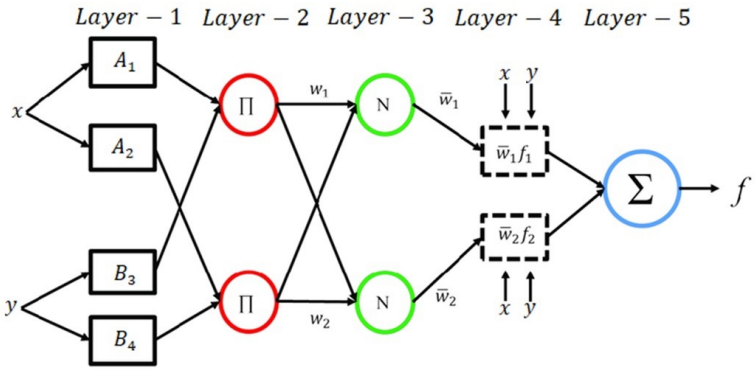

Figure 3. General structure of the Adaptive Neuro Fuzzy Inference System

2.1.1 *Layer-1*

The outputs of layer 1 are the fuzzy membership grade of the inputs, which are given by:

$$\begin{cases} o_i^1 = \mu_{A_i}(x) & i = 1,2 \\ o_i^1 = \mu_{B_i}(y) & i = 3,4 \end{cases} \tag{3}$$

where i is the node number, A_i and B_{i-2} are the linguistic labels associated with their respective node functions and μ_{A_i} and $\mu_{B_{i-2}}$ are the membership functions of the linguistic labels A_i and B_i respectively. Usually, the gbell function is chosen as membership function. The parameters in this layer are referred to as premise parameters.

2.1.2 *Layer-2*

Each i^{th} node outputs the firing strength of a rule defined as

$$o_i^2 = w_i = \mu_{A_i}(x) \cdot \mu_{B_{2+i}}(y), i = 1,2 \tag{4}$$

2.1.3 *Layer-3*

Every node i in this layer normalises the firing strength as follows

$$o_i^3 = \overline{w}_i = \frac{w_i}{w_1 + w_2}, i = 1,2 \tag{5}$$

2.1.4 *Layer-4*

The nodes in this layer are adaptive nodes with membership functions expressed as:

$$o_i^4 = \overline{w}_i f_i = \overline{w}_i \left(p_i x + q_i y + r_i\right), i = 1,2 \tag{6}$$

where $\overline{w}_i$ is a normalized firing strength from layer 3 and (p_i, q_i, r_i) is the consequent parameter set of node i.

2.1.5 *Layer-5*

This layer has a single node which computes the overall output as the sum of all incoming signals. The computation is represented as:

$$o_1^5 = \sum_i \overline{w}_i f_i, i = 1,2 \tag{7}$$

This is given by the following expression:

$$o_1^5 = (\overline{w}_1 x)\, p_1 + (\overline{w}_1 y)\, q_1 + (\overline{w}_1)\, r_1 + (\overline{w}_2 x)\, p_2 + (\overline{w}_2 y)\, q_2 + (\overline{w}_2)\, r_2 \tag{8}$$

During the training process, a hybrid training algorithm which adopts both forward and backward propagations is used. During the forward pass, the premise parameters are fixed while consequent parameters are updated and vice versa during the backward pass. The consequent parameters are updated with Least Square Estimate. The update of the premise parameters which is basically the fine tuning of the membership functions is done using Gradient Descent.

2.2 *Proposed ANFIS controller and training*

The proposed ANFIS controller adds the integral of Area Control Error (ACE) to the two traditional input signals consisting of the ACE and the derivative of ACE. ACE represents the discrepancy between scheduled and actual values of power and frequency, and the main function of the controller is to minimize the ACE. A hybrid of two trapezoidal and two gbell membership functions is selected for each input signal. The gbell membership functions offer flexibility in capturing nonlinear relationships and representing complex system dynamics, especially in scenarios involving renewable energy integration. The trapezoidal functions are used as outer membership functions to extend the range of outer crisp values which then enhance the overall system's flexibility. The combination allows the controller to effectively handle both linear and nonlinear aspects of the system, improving its adaptability and robustness. Not choosing gbell functions for all four membership functions also reduces the computational burden of the ANFIS controller. The training data is generated by applying ADIWACO-tuned PID controllers to the test system. Figure 4 shows the block diagram of the proposed ANFIS controller.

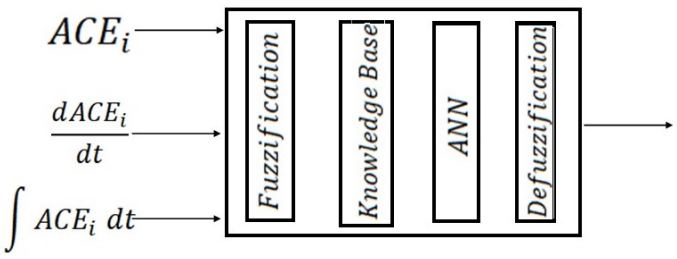

Figure 4. Proposed ANFIS Block Diagram

The Matlab *Anfisedit* toolbox is used for the ANFIS training. The training is implemented as follows:

Step 1: Model the test system in MATLAB/SIMULINK with ADIWACO-tuned PID controllers.

Step 2: Run a series of simulations using step load perturbations, with their magnitudes varying from 0.001 to 0.1 pu in increments of 0.001. Employ the "To Workspace" block to record the input ACE, the derivative of ACE and the integral of ACE as the input training dataset. Concurrently, capture the output from the PID controller to construct the output training dataset.

Step 3: Preprocess the captured dataset.

Step 4: Use 70% of the data for training and the remaining 30% for testing. Generate extra data with negative 0.05 pu step load perturbation for further testing of the controller after its training and successful initial testing.

Step 5: Employ the "*Anfisedit*" toolbox within Matlab to configure an ANFIS having three input variables and one output variable.

Step 6: Load the designated training dataset and proceed to generate a fuzzy inference system with four membership functions (MFs) for each input variable. Select the generalized bell-shaped membership functions, with the outermost MFs designated as trapezoidal membership functions.

Step 7: Train the ANFIS and test the performance against the reserved testing dataset. If performance is unsatisfactory, increase the number of epochs, try normalizing the dataset during the data preprocessing or generate new dataset as a final resort.

Step 8: If the test result is satisfactory, save the trained ANFIS.

The proposed ANFIS structure and input membership functions before and after the training are shown in Figures 5–11. The proposed ANFIS, unlike the traditional ANFIS for LFC, takes three inputs: ACE, the derivative of the ACE, and the integral of the ACE. The inclusion of the integral of the ACE accounts for the historical accumulation of the ACE, which leads to an improved control action. This enhancement ensures that the control system better addresses both current and past deviations in frequency, resulting in a more robust and responsive load frequency control.

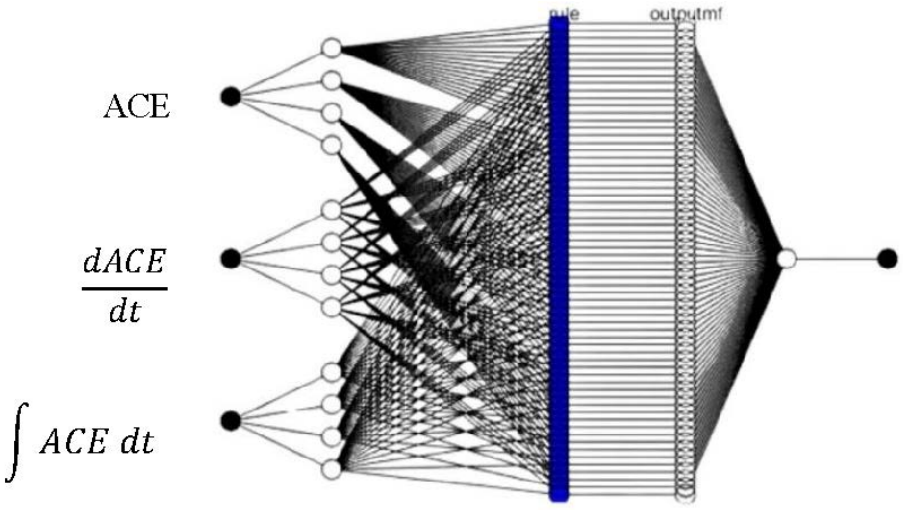

Figure 5. Proposed ANFIS Structure Showing all 5 Layers

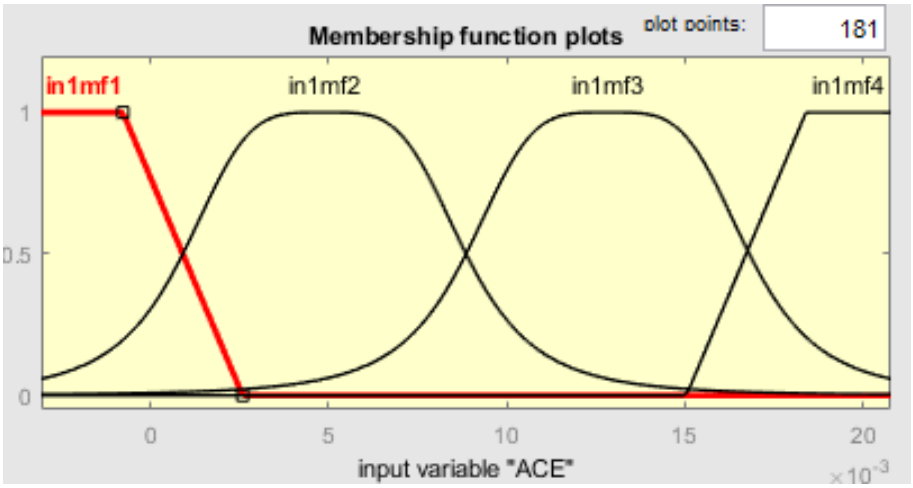

Figure 6. Membership functions for ACE input before training

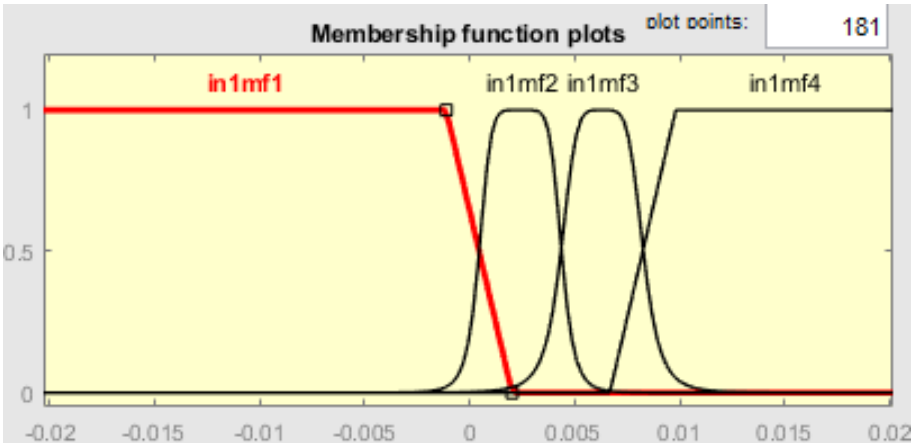

Figure 7. Membership functions for ACE input after training

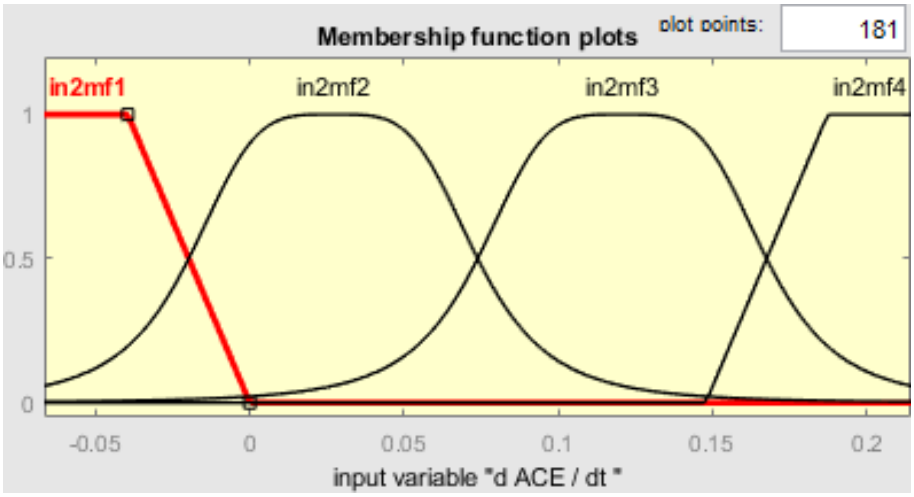

Figure 8. Membership functions for the derivative of ACE input before training

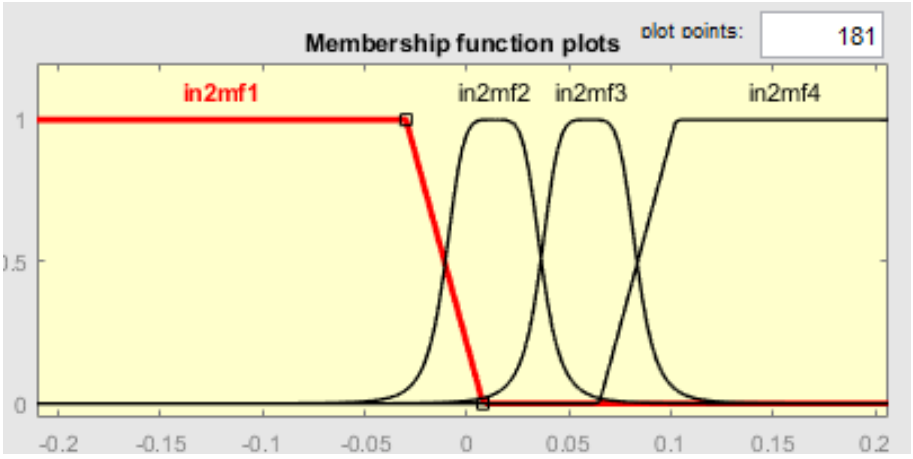

Figure 9. Membership functions for the derivative of ACE input after training

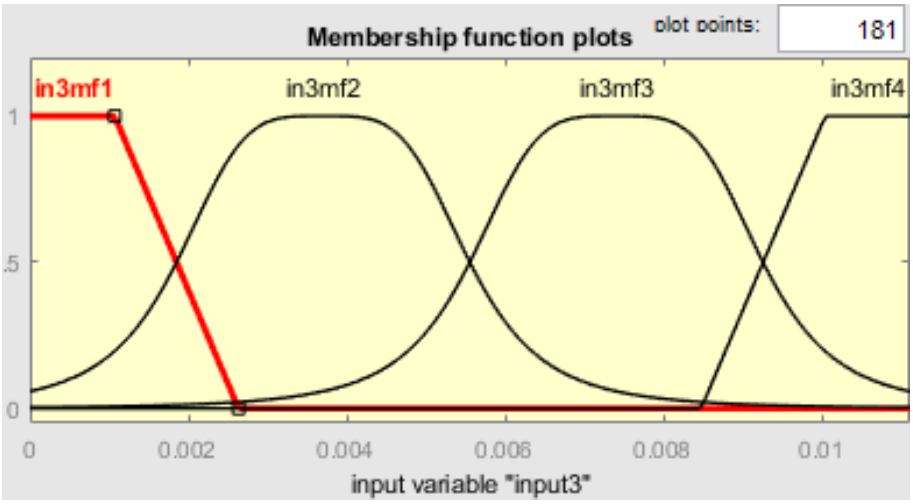

Figure 10. Membership functions for the integral of ACE input

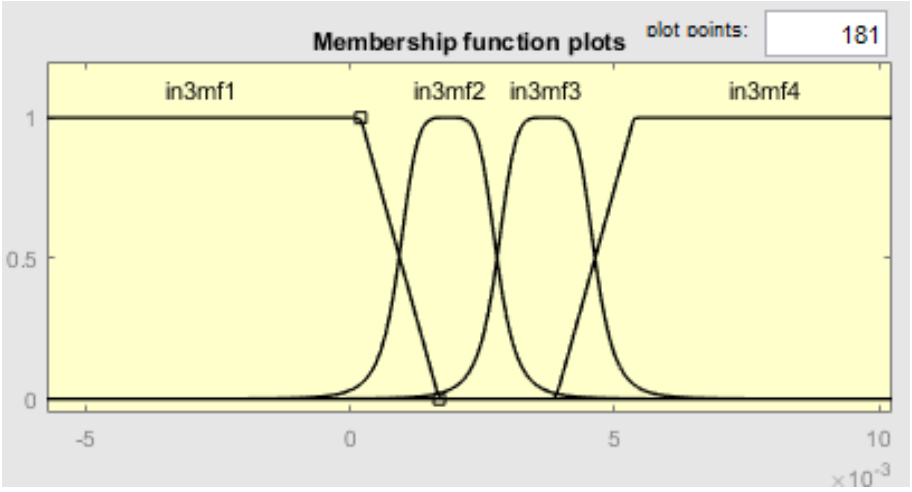

Figure 11. Membership functions for the integral of ACE input after training

Four membership functions are selected for each of the inputs. The two inner membership functions are chosen as generalized bell (gbell) membership functions, while the two outer membership functions are selected as trapezoidal membership functions. This combination strikes a balance between performance and computational complexity, optimizing the system's accuracy and efficiency. Figures 6–11 illustrate the membership functions of the three inputs both before training and after the membership function parameters have been updated following the final training epoch. These membership functions are given by (9) and (10).

$$\mu_{gbell}(x;a_i,b_i,c_i) = \frac{1}{1+\left|\frac{x-c_i}{a_i}\right|^{2b_i}} \tag{9}$$

where x is the input vector with crisp values to be converted to fuzzy values by the membership functions, a_i, b_i, c_i are parameters set that shape the membership functions. Specifically, c_i represents the center, a_i is half the width, and b_i determines the slope of the bell-shaped membership function. These parameters are updated during the backpropagation phase of the hybrid training algorithm for the ANFIS controller, allowing the system to learn and adapt for improved performance.

$$\mu_{trapezoidal}(x;a_i,b_i,c_i) = \begin{cases} 0, & x \le a_i \\ \frac{x-a_i}{b-a_i}, & a_i < x \le b_i \\ 1, & c_i < x \le d_i \\ \frac{x-a_i}{b_i-a_i}, & c_i < x \le d_i \\ 0, & x \ge a_i \end{cases} \tag{10}$$

where a_i and b_i define the feet, and c_i and d_i the shoulders of the trapezoid.

The Figure 12 illustrates the progression of the overall network error across training epochs. This graphical representation offers insight into the convergence behavior of the network during the training process. By tracking the fluctuations in error over successive epochs, the figure provides a visual depiction of how effectively the network learns and adjusts its parameters to minimize error and improve performance. Such visualizations play a crucial role in understanding the dynamics of the training process and assessing the efficacy of the employed training algorithm or model architecture.

Figure 12 shows the progression of the overall neural network error across training epochs. The figure provides a visual depiction of how the neural network learns and adjusts its parameters to minimize error and improve performance and hence an indication of the efficacy of the employed training algorithm or model architecture.

Figure 13 shows the performance of the ANFIS controller when tested against the training dataset. The blue circles represent the training data while the red stars represent the output of the ANFIS controller. A close match between the two suggests effective learning. The figure depicts the effectiveness of the ANFIS controller to capture patterns and relationships within the data that it was trained on. Figure 14 is the same as Figure 12 except that the testing of the controller is against an unseen dataset. The unseen dataset is generated by ADIWACO-tuned PID controller following the application of a negative 0.05 per unit step load perturbation to the test system. Figure 14 validates the generalization ability of the ANFIS controllers outside of their training dataset.

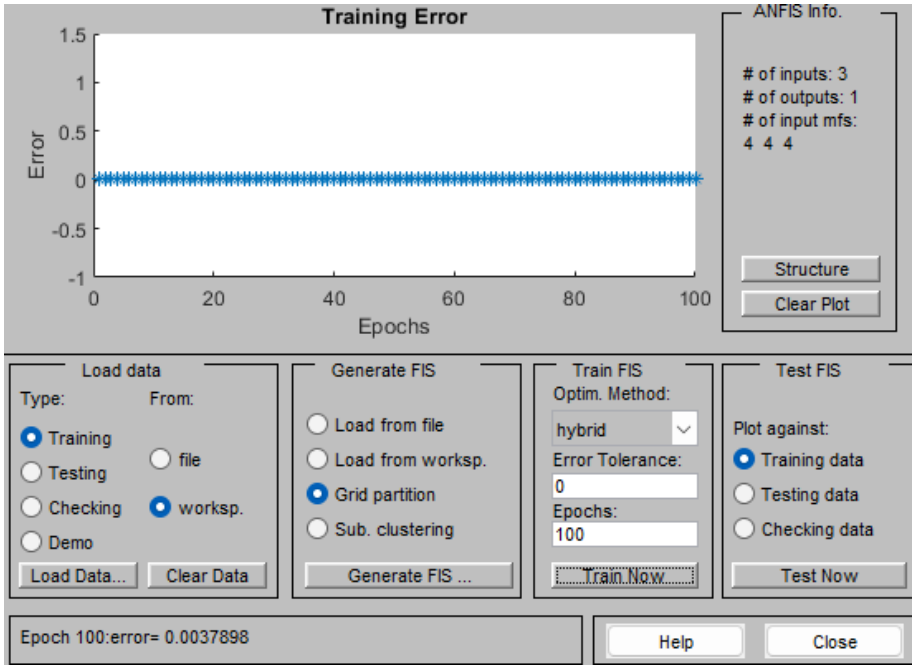

Figure 12. Progression of the overall neural network error across training epochs

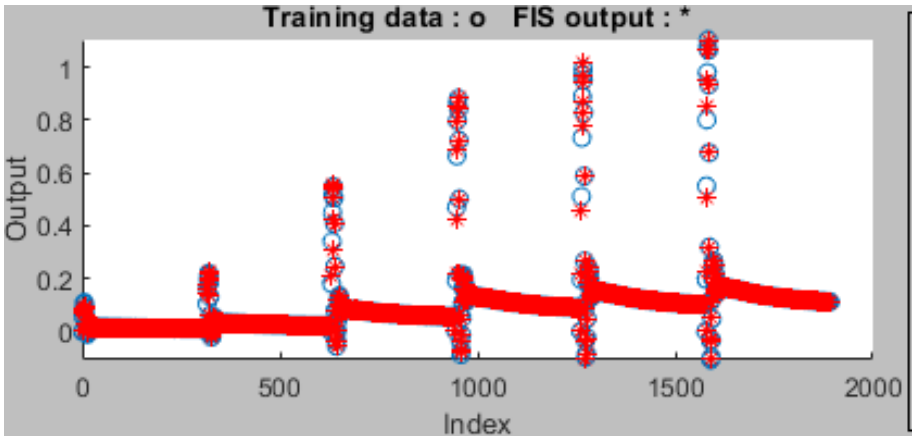

Figure 13. Performance of the ANFIS model when tested against the training dataset

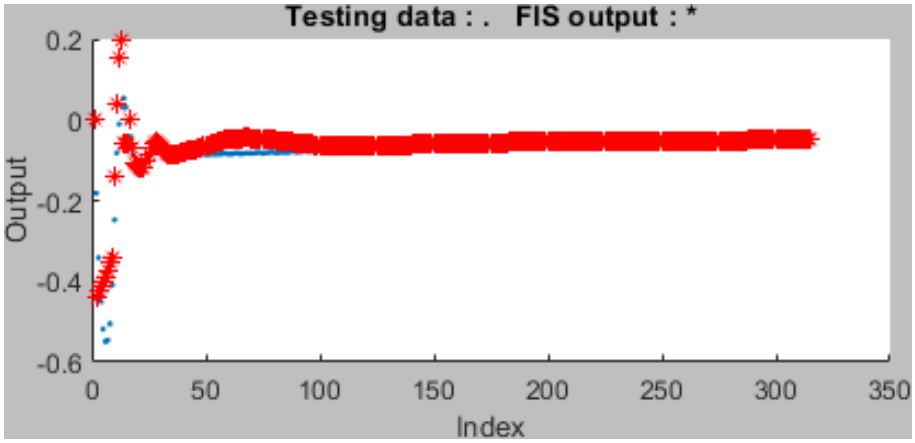

Figure 14. Performance of the ANFIS model when tested against an unseen dataset

2.3 *Testing the proposed controller on the test system*

The efficacy of the proposed ANFIS controller for load frequency control is tested on the test system using Matlab/Simulink (R2023a) environment. The laptop for the implementation has Windows 11 (64-bit) edition and is equipped with Intel(R) Core (TM) i5-8250U CPU @ 1.60 GHz 1.80 GHz and installed RAM of 24.0 GB. Four distinct experimental scenarios, detailed in the subsequent section, are executed to assess the controller's performance. The performance evaluation is done in terms of the following performance metrics: settling time, steady state error, overshoot, undershoot, and integral time absolute error (ITAE) values. A comparative analysis is performed against four existing LFC strategies, namely LFC strategies based on ADIWACO-tuned PID controller [3], fuzzy logic controller employing the fuzzy rule set proposed in [22], an ANN-based controller in [49], and an ANFIS controller with only ACE and its derivative as inputs proposed in [24]. This ANFIS controller is termed "Traditional ANFIS controller" throughout this paper. The Simulation model and the controller subsystem within the simulation model are presented in Figures 15 and 16 respectively.

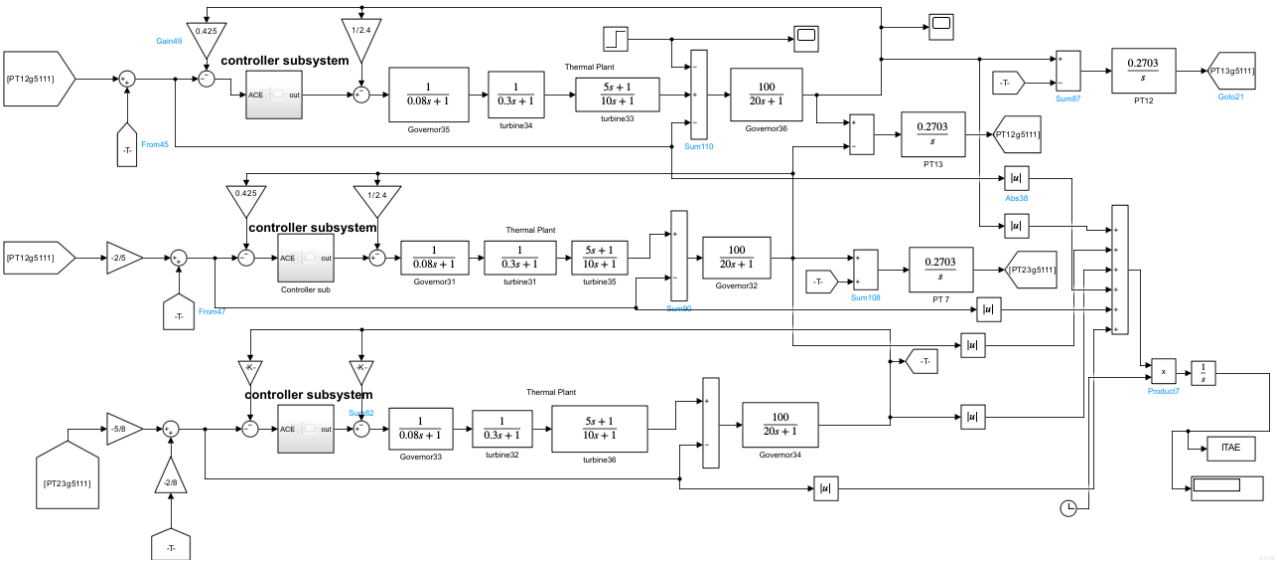

Figure 15. Simulation model of the test system

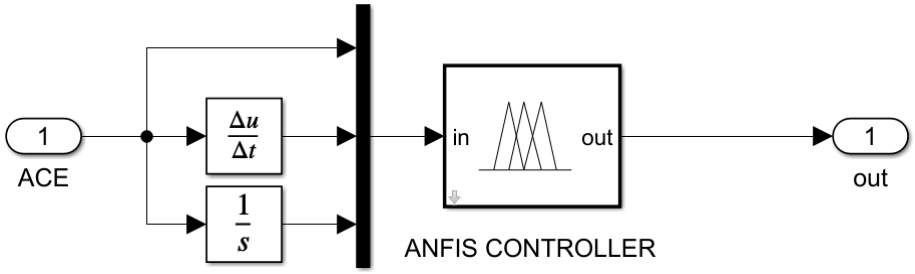

Figure 16. Controller subsystem within the simulation model

3. Results and discussion

3.1 *Scenario 1*

In this experimental scenario, a perturbation consisting of a positive step load of 0.1 is applied in area 1 of the test system. The comparison curves of the frequencies and the tie-line power flows are shown in Figures 17–22. The corresponding ITAE values and relevant waveform characteristics are given in Table 1. From Table 1, regarding the settling time of the frequency response of Area 1, the proposed ANFIS controller emerges as the best, recording the shortest settling time of an impressive 2.1 s. This represents a substantial improvement of 81.25% (11.2 s), 84.5588% (13.6 s), and 48.7805% (4.1 s) in comparison to the settling times provided by the ANN, Fuzzy Logic, and Traditional ANFIS controllers respectively. It is worth noting that the ADIWACO-tuned PID controller demonstrated competitive performance with a settling time of 2.3 s (8.696%). Similar improvements are observed regarding the frequency responses of areas 2 and 3, and power responses in the tie lines.

Also, in terms of undershoot and overshoot in the tie lines power and frequency responses, the proposed ANFIS controller shows superior performance to the comparison controllers. For Area 1 frequency response, the proposed controller exhibits an undershoot of 0.041 Hz which represents 14.58% (0.048 Hz), 46.05% (0.076 Hz), 83.8583% (0.254 Hz) and 10.8696% (0.046 Hz) improvement on the PID, ANN, Fuzzy Logic and the Traditional ANFIS controllers respectively. This observation does not differ too much for the frequency responses of the other control areas and the tie-line power responses. The proposed ANFIS controller provides frequency and tie lines power responses with zero overshoot for all areas except area 1 frequency response which has an overshoot of 0.0051 Hz. This is only excelled by the Traditional ANFIS controller which produces area 1 frequency response with no overshoot.

In terms of steady state error, both the PID and the proposed ANFIS controllers yield approximately zero errors in both the frequency and the tie lines power responses of all the control areas. The Traditional ANFIS controller provides comparable steady-state error performance, with the steady state error not exceeding 0.014 in all cases. In contrast, the ANN and fuzzy logic controllers give larger steady-state errors.

Regarding the ITAE values, the proposed ANFIS controller produces the lowest value of 0.04932, signifying superior overall performance in mitigating deviations of the area frequencies and tie-line power flows. The Traditional ANFIS and PID controllers exhibit competitive ITAE values. The improvement in their ITAE values by the proposed ANFIS controller are 18.4928% (0.06051) and 21.2141% (0.0626) respectively. The ANN and fuzzy logic controllers yield higher ITAE values, indicating suboptimal control performance.

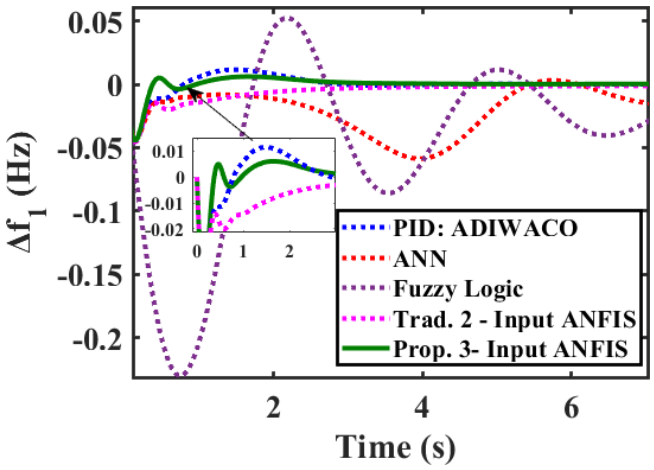

Figure 17. Scenario 1 Area 1 frequency response

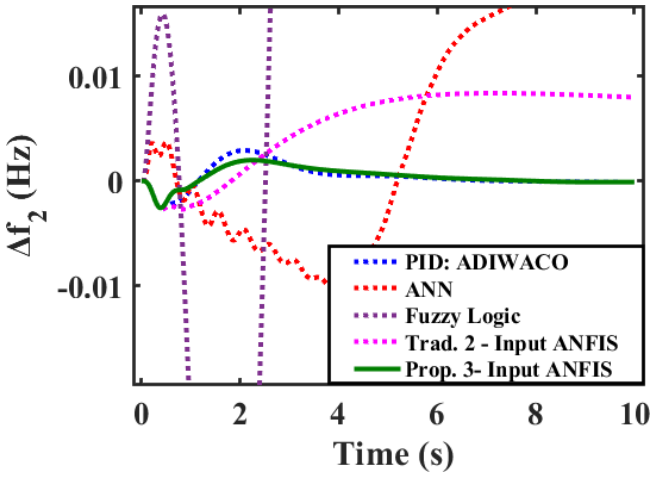

Figure 18. Scenario 1 Area 2 frequency response

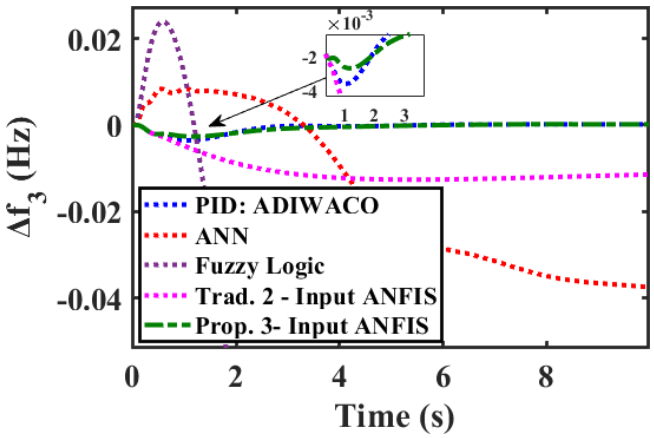

Figure 19. Scenario 1 Area 3 frequency response

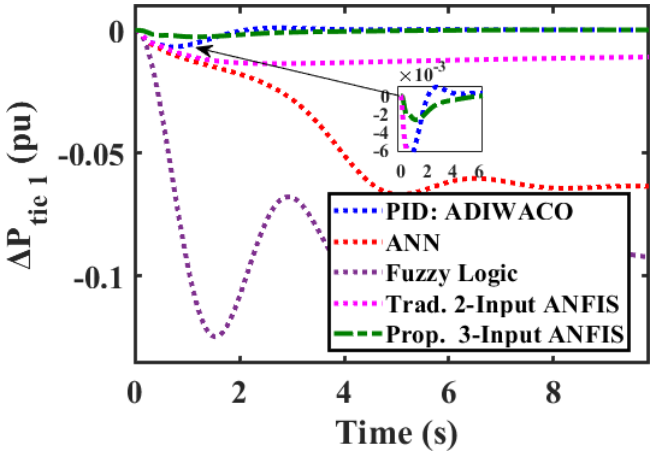

Figure 20. Scenario 1 $\Delta P_{(tie\ 1)}$

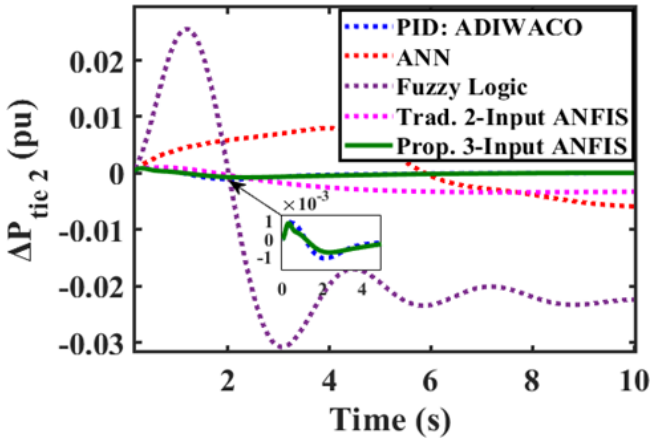

Figure 21. Scenario 1 $\Delta P_{(tie\ 2)}$

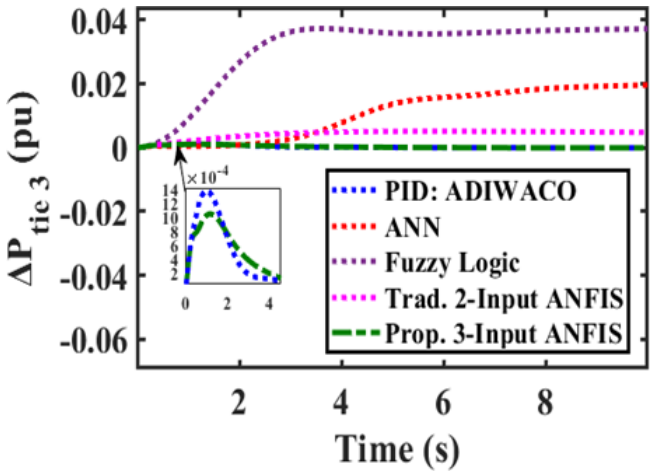

Figure 22. Scenario 1 $\Delta P_{(tie\ 3)}$

Table 1. Scenario 1 results (left)

Controller	Settling Time (s)			Undershoot (−ve Hz)			Overshoot (Hz)		
	Δf_1	Δf_2	Δf_3	Δf_1	Δf_2	Δf_3	Δf_1	Δf_2	Δf_3
PID	2.3	**2.9**	1.7	0.048	**0.002**	0.004	0.011	**0**	**0**
ANN	11.2	9.4	10.4	0.076	0.011	0.042	0.035	0.004	0.008
Fuzzy Logic	13.6	18.4	12.2	0.254	0.091	0.144	0.052	0.129	0.024
Trad. ANFIS	4.1	6.1	4.2	0.046	0.004	0.013	**0**	**0**	**0**
Prop. ANFIS	**2.1**	**2.9**	**1.6**	**0.041**	**0.002**	**0.002**	0.0051	**0**	**0**

Table 1. Scenario 1 results (right)

Undershoot (−ve puMW)			Steady State Error (f in Hz, P in pu)						ITAE Values
ΔP_1	ΔP_2	ΔP_3	Δf_1	Δf_2	Δf_3	ΔP_1	ΔP_2	ΔP_3	
0.006	**0.001**	**0**	**0**	**0**	**0**	**0**	**0**	**0**	0.06051
0.078	**0**	**0**	0.002	0.02	−0.04	−0.081	−0.004	0.023	1.097
0.138	0.035	**0**	0.01	0.04	−0.11	−0.095	−0.031	0.051	0.3925
0.009	**0.003**	**0**	**0**	0.01	−0.01	−0.014	−0.004	0.001	0.0626
0.002	**0.001**	**0**	**0**	**0**	**0**	**0**	**0**	**0**	**0.04932**

3.2 *Scenario 2*

This scenario tests the controller in a dynamic environment by applying simultaneously random load perturbation, wind turbine power generation, and solar power generation disturbances in Area 1 of the test system. The applied disturbance, shown in Figure 23, is what is applied in the study reported in [3, 36]. The results, in terms of the performance metrics used in scenario 1 except for the settling time and steady state errors, presented in Figures 24–29 and Table 2, offer a comprehensive insight into the controllers' performance under these challenging conditions. The proposed ANFIS controller proves superior in most cases to the comparison LFC controllers regarding overshoot and undershoot in the responses of area frequencies and tie-line power flows. Notably, in the response of area 1 frequency, an overshoot of 0.01 Hz is obtained, representing a 66.66% (0.01 Hz), 91.67 % (0.12 Hz), 93.75% (0.16 Hz) and 83.33 % (0.06 Hz) improvement over the overshoots provided by the PID, ANN, fuzzy logic and the Traditional ANFIS controllers respectively. The Traditional ANFIS controller provides an overshoot value of zero in area 3 frequency response. However, its corresponding undershoot value of 0.015 Hz is the worst of the values produced by all five controllers. The undershoot value of 0.001 Hz by the proposed ANFIS controller represents an improvement of 93.33% over this value. Once again in terms of the ITAE value, which provides a measure of the overall efficacy of a controller to mitigate frequency and tie-line power deviations, the proposed controller maintains the lowest ITAE value of 0.1116. The ITAE value represents an improvement of 13.3% (0.1338), 90.02% (1.163), 77.81% (0.5227) and 76.51% (0.4939) over the corresponding values of the PID, ANN, Fuzzy Logic and the Traditional ANFIS controllers respectively. Scenario 2 results highlight the efficacy of the proposed ANFIS controller in mitigating the impact of severe power system disturbances.

Table 2. Scenario 2 results

Controller	Overshoot (Hz)			Undershoot (−ve Hz)			Overshoot (pu MW)			Undershoot (−ve pu MW)			ITAE Values
	Δf_1	Δf_2	Δf_3	Δf_1	Δf_2	Δf_3	ΔP_1	ΔP_2	ΔP_3	ΔP_1	ΔP_2	ΔP_3	
PID	0.03	0.003	0.001	0.010	0.002	0.003	0.004	**0**	0	0.004	**0**	**0**	0.1338
ANN	0.12	0.007	0.005	**0.004**	0.018	0.015	0.01	0.012	0	0.001	**0**	0.007	1.163
Fuzzy Logic	0.16	0.211	0.019	0.144	0.024	0.12	0	**0**	0.04	0.246	0.165	0	0.5227
Trad. ANFIS	0.06	0.009	**0**	0.027	**0.001**	0.015	0	**0**	0	0.017	0.005	0.013	0.4939
Prop. ANFIS	**0.01**	**0.001**	0.001	0.011	0.002	**0.001**	**0.001**	**0**	**0**	0.004	**0**	**0**	**0.1116**

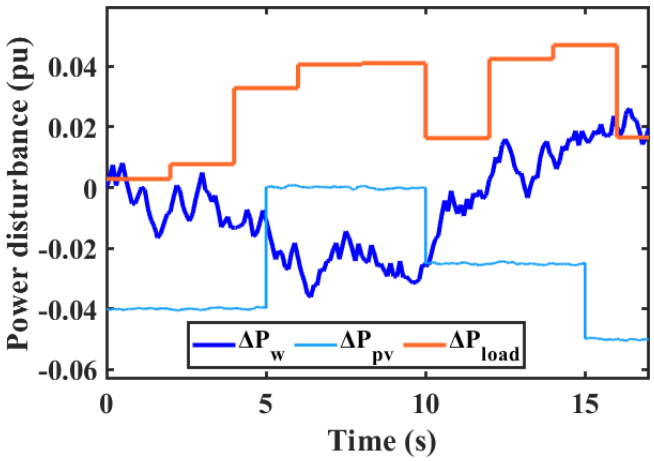

Figure 23. The applied power disturbances

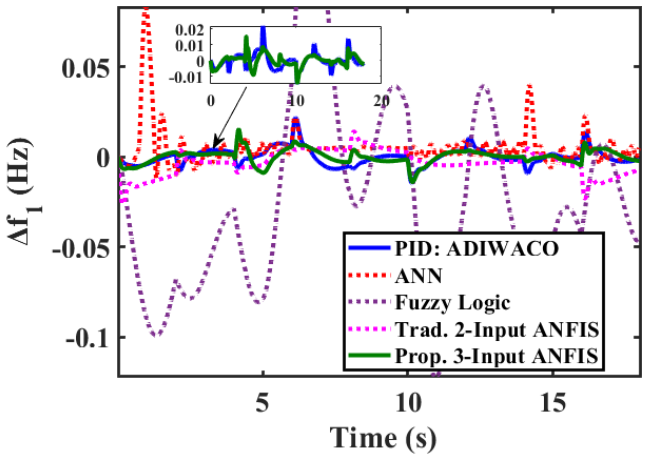

Figure 24. Scenario 2 Area 1 frequency response

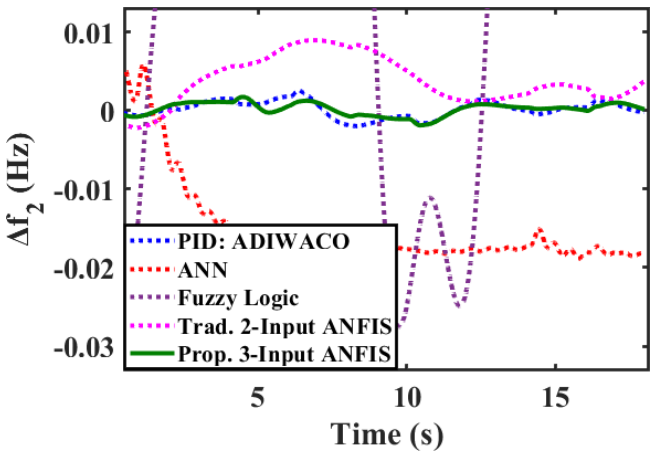

Figure 25. Scenario 2 Area 2 frequency response

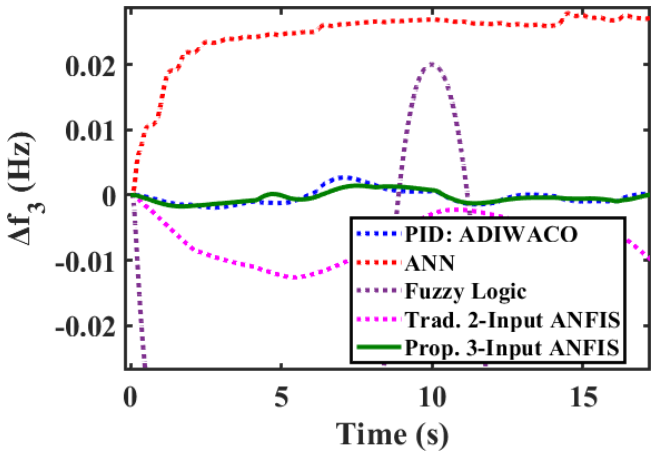

Figure 26. Scenario 2 Area 3 frequency response

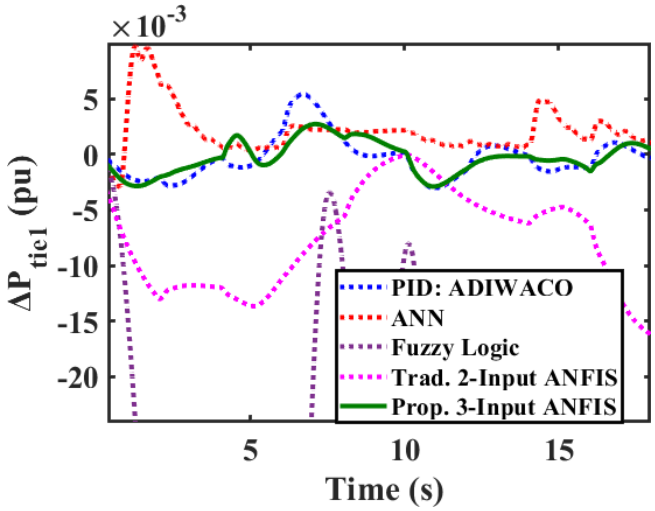

Figure 27. Scenario 2 $\Delta P_{(tie\ 1)}$

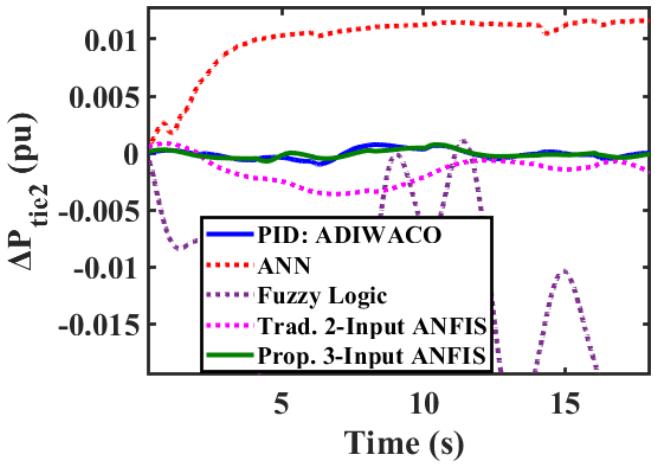

Figure 28. Scenario 2 $\Delta P_{(tie\ 2)}$

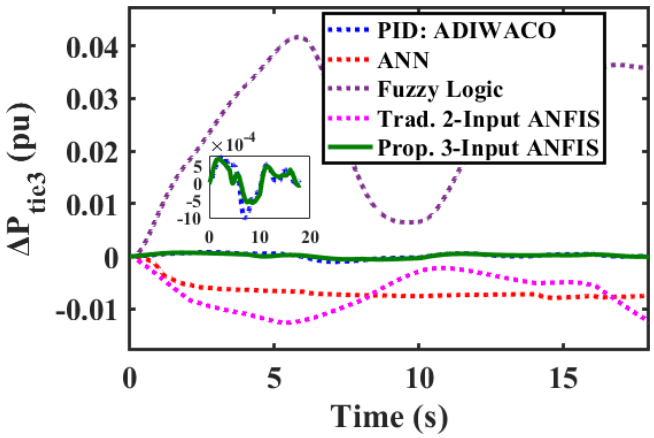

Figure 29. Scenario 2 $\Delta P_{(tie\ 3)}$

3.3 *Scenario 3*

This scenario is the same as Scenario 2 except that a governor dead band of 0.15 mHz and a communication time delay of 5 ms are factored into the power system model for more realistic performance evaluation as in [3]. The block diagram representation of the constraints which is incorporated in the power system model presented in Figure 1 is shown in Figure 30.

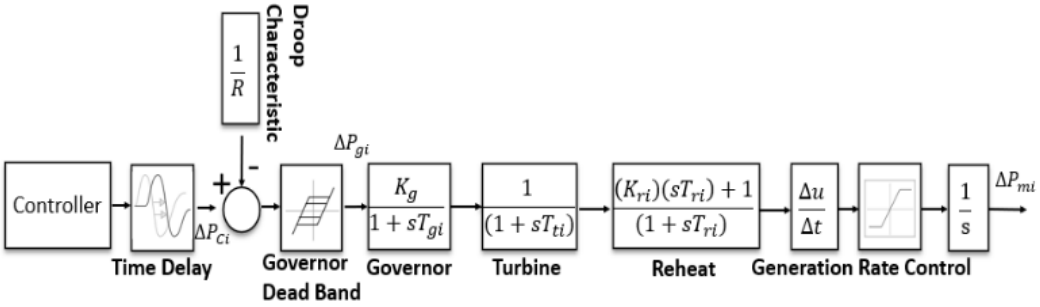

Figure 30. Block diagram representation of constraints

The results are presented in Figures 31–36 and Table 3. As shown by the results, the proposed ANFIS controller continues to demonstrate excellent performance, with minimal overshoot and undershoot in the presence of real-world physical constraints. Conversely, the fuzzy logic and ANN controllers produce increased overshoot and undershoot values, suggesting challenges in adapting to the combined disturbances and system constraints. The Traditional ANFIS and the PID controllers maintain competitive performance, with the proposed ANFIS showing marginal improvements, particularly in keeping down overshoot. Regarding ITAE value, the proposed controller still provides the lowest value of 0.1388. The fuzzy logic and ANN controllers give higher ITAE values, indicating inferior performance in the presence of the two physical constraints. The proposed ANFIS controller improves their ITAE values by 97.06% (4.807) and 99.99% (176) respectively.

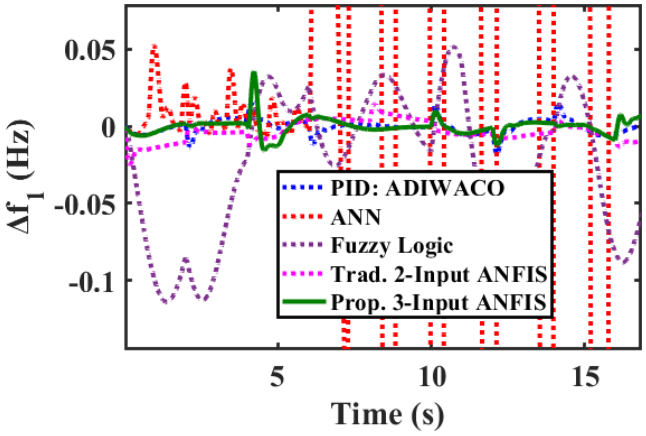

Figure 31. Scenario 3 Area 1 frequency response

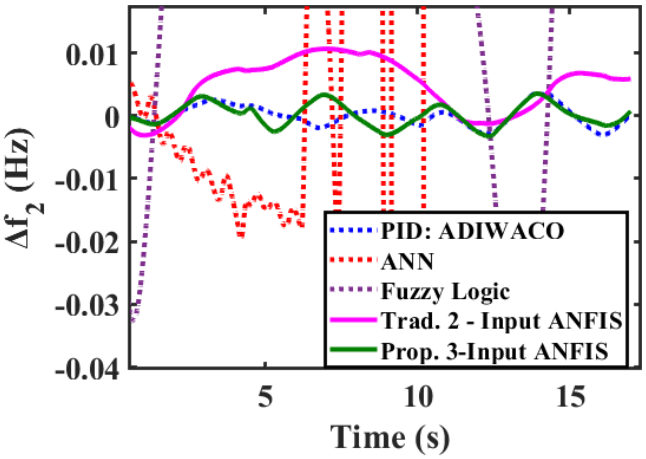

Figure 32. Scenario 3 Area 2 frequency response

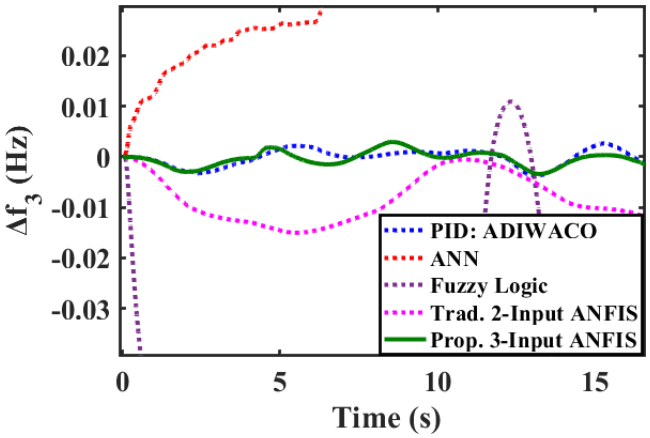

Figure 33. Scenario 3 Area 3 frequency response

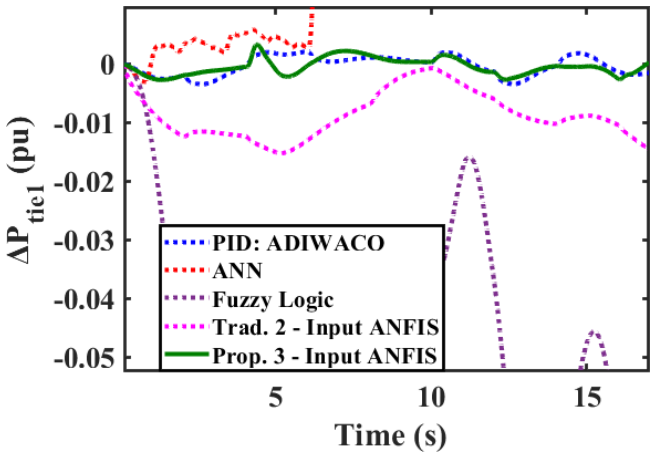

Figure 34. Scenario 3 $\Delta P_{(tie\ 1)}$

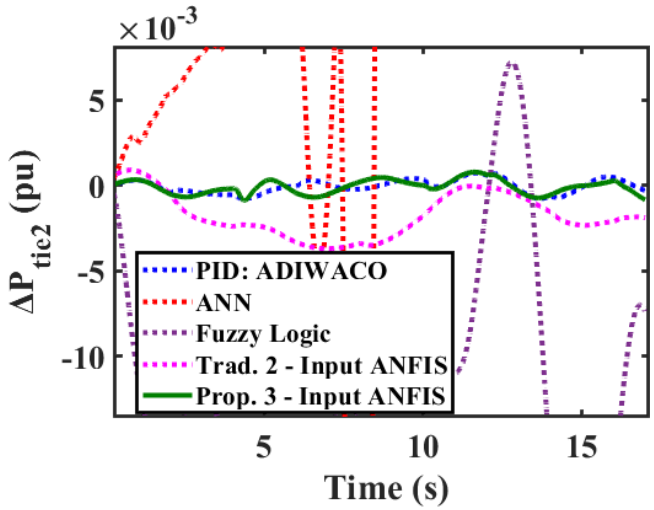

Figure 35. Scenario 3 $\Delta P_{(tie\ 2)}$

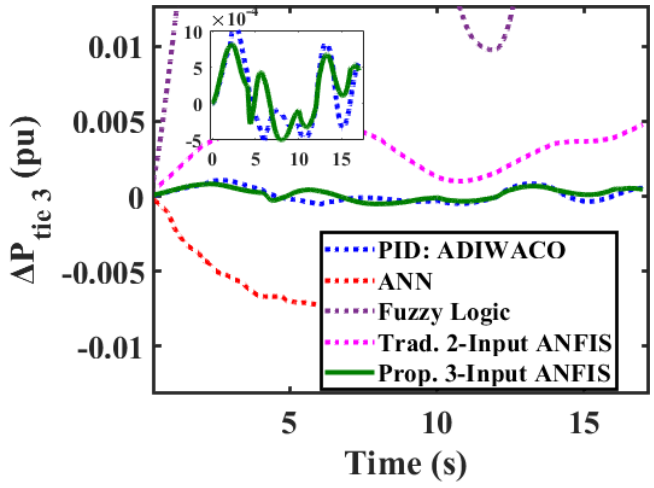

Figure 36. Scenario 3 $\Delta P_{(tie\ 3)}$

Table 3. Scenario 3 results

Controller	Overshoot (Hz)			Undershoot (−ve Hz)			Overshoot (Hz)			Undershoot (−ve pu MW)			ITAE Values
	Δf_1	Δf_2	Δf_3	Δf_1	Δf_2	Δf_3	ΔP_1	ΔP_2	ΔP_3	ΔP_1	ΔP_2	ΔP_3	
PID	**0.01**	0.0023	0.003	**0.01**	0.004	0.003	0.002	**0**	0.0012	**0.002**	**0**	0.0005	0.1411
ANN	0.22	0.03	0.03	0.24	0.03	**0**	0.355	0.01	0	0.002	0.141	0.0073	176.2
Fuzzy Logic	0.05	0.28	0.01	0.12	0.24	0.04	**0**	0.0001	0	0.411	0.386	0.4951	4.807
Trad. ANFIS	0.02	0.01	**0**	0.03	**0.003**	0.031	**0**	0.0001	0.005	0.015	0.004	**0**	0.5749
Prop. ANFIS	0.03	**0.002**	0.002	0.02	**0.003**	0.003	0.002	**0**	**0.0007**	**0.002**	**0**	0.0005	**0.1388**

3.4 *Scenario 4*

In Scenario 4, system parameters are varied by ±25% to verify the robustness of three of the controllers: the proposed ANFIS controller, the PID controller, and the Traditional ANFIS controller. A step load perturbation of 0.05 pu is applied, and the ensuing results are presented in Table 4 and in Figures 37 and 38. From the curves, the proposed ANFIS and PID controllers demonstrate better robustness. Regarding ITAE, the proposed controller provides the lowest value of 0.0239 for the +25% parameters variation and 0.03708 for the −25% parameters variation as presented in Table 4, making it the best of the three under uncertain system model parameters.

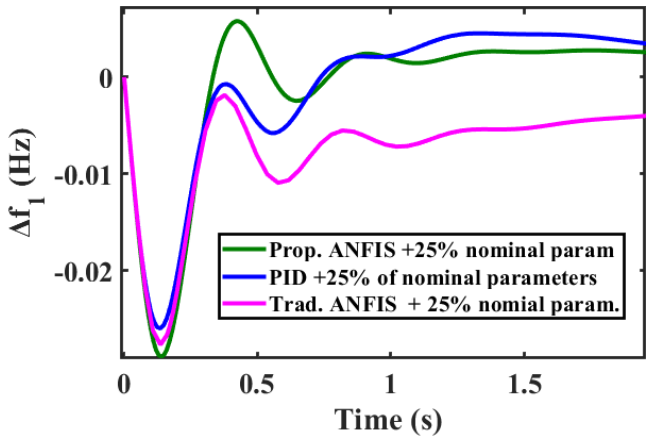

Figure 37. +25% of nominal parameters variation for Area 1 frequency response

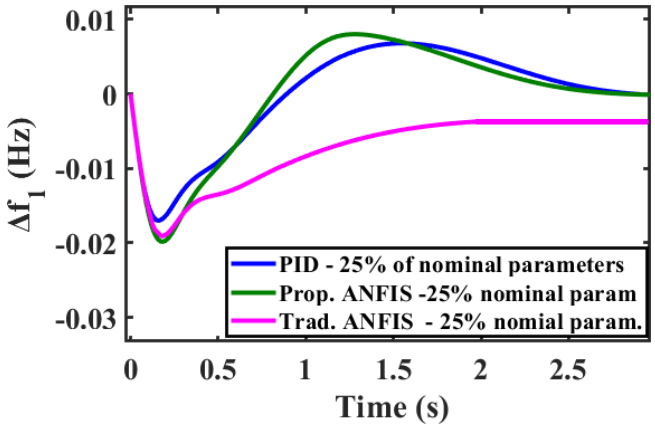

Figure 38. −25% of nominal parameters variation for Area 1 frequency response

Table 4. Scenario 4 results

Controller	+25% Parameter Variation	−25% Parameter Variation
	ITAE Values	ITAE Values
PID	0.02627	0.05413
Traditional ANFIS	0.13064	0.184
Proposed ANFIS	**0.0239**	**0.03708**

4. Conclusions

This paper has proposed a novel ANFIS controller for LFC in a multi-area power system with RES. The proposed ANFIS controller, improved by ading the integral of the ACE to its two traditional input signals consisting of ACE and derivative of ACE, has been systematically evaluated against four established controllers: PID, ANN, fuzzy logic, and ANFIS with the two traditional input signals on the IEEE-39 bus test system modified as a three-area power system with RES integration. The training dataset of the proposed ANFIS is generated by PID controllers tuned by a variant of PSO algorithm called ADIWACO. Through four experimental scenarios involving disturbances and real-world power system constraints- specifically communication time delays and governor dead bands-, performance metrics comprising settling time, overshoot, undershoot, steady-state error, and ITAE values, have been rigorously analyzed. The results demonstrate that the performance of the proposed ANFIS controller is superior in all four scenarios. Particularly, it gives a far lower settling time than the comparison controllers when a positive step load perturbation of 0.1 is applied in the first experimental scenario and the lowest ITAE values across all the experimental scenarios. Notably, the proposed ANFIS controller shows a 75.89% improvement in ITAE value over the traditional 2-input ANFIS when implemented in a RES-integrated power system with communication delays and governor dead band constraints, underscoring the importance of the additional input. Also, variation of power system parameters in one experimental scenario further highlights the robustness of the proposed controller to uncertain system model parameters. As power systems continue to evolve, the adaptability and robustness demonstrated by the proposed ANFIS controller make it a viable choice for efficient and resilient load frequency control strategy in multi-area power systems with RES.

Appendix

Test system: Area 1 rating = 820 MW, Area 2 rating = 2050 MW, Area 3 rating = 3280 MW, nominal loading = 50%, area power rating ratios $\alpha_{12} = -\frac{2}{5}, \alpha_{13} = -\frac{2}{8}, \alpha_{23} = -\frac{5}{8}$, Kps = 100, Power system time constant = 20 s, Droop Constant (1/R) = 0.333 p.u.MW/Hz, Frequency Bias, B_1 = 0.425 p.u.MW/Hz, Synchronization coefficient, T = 0.545, Solar PV generation participation factor 0.33, Wind generation participation factor 0.33, Thermal plant participation factor 0.33. Solar PV generation rating = 273.3 MW, Solar PV time constant, T_{PV} = 1.8 s, Solar PV gain, K_{PV} = 1, Wind Turbine generation rating = 273.3 MW, Wind Turbine generation participation factor 0.33, Wind generation time constant, T_{WTG} = 1.5 s, Wind turbine generation gain, K_{WTG} = 1, Droop Constant (1/R) = 0.417 p.u.MW/Hz, Frequency Bias, B = 0.425 p.u.MW/Hz. Governor gain K_g = 1, Governor time constant, T_g = 0.08, Turbine gain, K_t = 1, Turbine time constant T_t = 0.3, Thermal reheater time constant, T_{re} = 10, Thermal reheater gain, K_{re} = 0.5.

$$\begin{aligned}\Delta P_{tie,1} &= \Delta P_{tie,12} + \Delta P_{tie,13},\\ \Delta P_{tie,2} &= \alpha_{12}\Delta P_{tie,12} + \Delta P_{tie,23},\\ \Delta P_{tie,3} &= \alpha_{13}\Delta P_{tie,13} + \alpha_{23}\Delta P_{tie,23}\end{aligned}$$

Author contributions

We hereby affirm that the collaborative efforts of YOMS, FBE, and PYO were instrumental in the design and implementation of this research. YOMS, FBE, and PYO played key roles in analyzing the results and writing the manuscript. Every named author has thoroughly reviewed and approved of the final manuscript.

Conflict of interest

The authors of the current study declare that they have no competing interests.

References

[1] H. Shayeghi, I. F. Davoudkhani, and N. Bizon, "Robust self-adaptive fuzzy controller for load-frequency control of islanded airport microgrids considering electric aircraft energy storage and demand response," *IET Renew. Power Gener.*, vol. 18, no. 4, pp. 616–653, 2024, doi: 10.1049/rpg2.12926.

[2] Y. O. M. Sekyere, F. B. Effah, and P. Y. Okyere, "Optimally tuned cascaded FOPI-FOPIDN with improved PSO for load frequency control in interconnected power systems with RES," *J. Electr. Syst. Inf. Technol.*, vol. 11, no. 1, p. 25, Jul. 2024, doi: 10.1186/s43067-024-00149-x.

[3] Y. O. M. Sekyere, F. B. Effah, and P. Y. Okyere, "Optimal Tuning of PID Controllers for LFC in Renewable Energy Source Integrated Power Systems Using an Improved PSO," *J. Electron. Electr. Eng.*, vol. 3, no. 1, pp. 65–83, Jan. 2024, doi: 10.37256/jeee.3120243869.

[4] Y. V. Hote and S. Jain, "PID controller design for load frequency control: Past, Present and future challenges," *IFAC-PapersOnLine*, vol. 51, no. 4, pp. 604–609, 2018, doi: 10.1016/j.ifacol.2018.06.162.

[5] D. Sharma, "Load Frequency Control: A Literature Review," *Int. J. Sci. Technol. Res.*, vol. 9, no. 2, pp. 6421–6437, 2020.

[6] H. K. Shaker, H. El Zoghby, and M. E. Bahgat, "Advanced Control Techniques for an Interconnected Multi Area Power System for Load Frequency Control," in *Proc. 2019 21st Int. Middle East Power Syst. Conf.*, Cairo, Egypt, Dec. 17–19, 2019, pp. 710–715.

[7] M. Ahmed, M. Khamies, G. Magdy, and S. Kamel, "Designing Optimal $PI^{\lambda}D^{\mu}$Controller for LFC of Two-Area Power Systems Using African Vulture's Optimization Algorithm," in *Proc. 22nd Int. Middle East Power Syst. Conf. MEPCON 2021*, Assiut, Egypt, Dec. 14–16, 2021, pp. 430–437, doi: 10.1109/MEPCON50283.2021.9686297.

[8] A. Latif, S. M. S. Hussain, D. C. Das, T. S. Ustun, and A. Iqbal, "A review on fractional order (FO) controllers' optimization for load frequency stabilization in power networks," *Energy Reports*, vol. 7, pp. 4009–4021, 2021, doi: 10.1016/j.egyr.2021.06.088.

[9] K. Gottapu, D. P. Chennamsetty, K. K. Isukapalli, P. K. Gorle, S. Nakka, and D. P. Chinta, "Load Frequency Control of Interconnected Power System with Renewables using Improved Fractional Integral Controller," *Int. J. Renew. Energy Res.*, vol. 13, no. 1, pp. 392–400, 2023, doi: 10.20508/ijrer.v13i1.13561.g8691.

[10] G. A. Suyasno, L. M. Putranto, M. Isnaeni Bambang Setyonegoro, S. Isnandar, and D. Y. Himawan, "Frequency Stability Consideration for Optimum Penetration of Renewable Energy: A Case of Southern Sulawesi System," in *Proc. ICT-PEP 2021—Int. Conf. Technol. Policy Energy Electr. Power Emerg. Energy Sustain. Smart Grid, Microgrid Technol. Futur. Power Syst.*, Jakarta, Indonesia, Sept. 29–30, 2021, pp. 366–371, doi: 10.1109/ICT-PEP53949.2021.9600999.

[11] D. Mishra, P. C. Nayak, S. K. Bhoi, and R. C. Prusty, "Grey wolf optimization algorithm based cascaded PID controller for Load-frequency control of OFF-Grid Electric Vehicle integrated Microgrid," in *Proc. 2020 IEEE Int. Symp. Sustain. Energy, Signal Process. Cyber Secur. iSSSC 2020*, Gunupur Odisha, India, Dec. 16–17, 2020, doi: 10.1109/iSSSC50941.2020.9358884.

[12] S. Prakash and S. K. Sinha, "Intelligent PI control technique in four area load frequency control of interconnected hydro-thermal power system," in *Proc. 2012 Int. Conf. Comput. Electron. Electr. Technol. ICCEET 2012*, Nagercoil, India, Mar. 21–22, 2012, pp. 145–150, doi: 10.1109/ICCEET.2012.6203749.

[13] D. Guha, P. K. Roy, and S. Banerjee, "Load frequency control of interconnected power system using grey Wolf optimization," *Swarm Evol. Comput.*, vol. 27, pp. 97–115, 2016, doi: 10.1016/j.swevo.2015.10.004.
[14] U. Bose, S. K. Chattopadhyay, C. Chakraborty, and B. Pal, "A novel method of frequency regulation in microgrid," *IEEE Trans. Ind. Appl.*, vol. 55, no. 1, pp. 111–121, 2019, doi: 10.1109/TIA.2018.2866047.
[15] B. S. Lokasree, Kirathan, E. Sagar, and M. M. Sakhib, "Robust Cascade Controller for Load Frequency Control of A Standalone Microgrid," in *Proc. 4th Int. Conf. Cybern. Cogn. Mach. Learn. Appl. ICCCMLA 2022*, Goa, India, Oct. 8–9, 2022, pp. 179–183, doi: 10.1109/ICCCMLA56841.2022.9989312.
[16] S. Panda, N. P. Patidar, and M. Kolhe, "Cascaded PD-PI controller for active power frequency control of two-Area multi-units power system," in *Proc. 2016 IEEE Int. Conf. Power Renew. Energy, ICPRE 2016*, Shanghai, China, Oct. 21–23, 2016, pp. 251–254, 2017, doi: 10.1109/ICPRE.2016.7871210.
[17] S. Pahadasingh, "TLBO based CC-PID-TID controller for load frequency control of multi area power system," in *Proc. 1st Odisha Int. Conf. Electr. Power Eng. Commun. Comput. Technol. ODICON 2021*, Bhubaneswar, India, Jan. 8–9, 2021, pp. 1–7, 2021, doi: 10.1109/ODICON50556.2021.9429022.
[18] P. Satapathy, "PDPID Plus DDF Cascaded Controller for LFC Investigation in Unified System with Wind Generating Unit," Bhubaneswar, India, Jan. 8–9, 2021, pp. 6–11, doi: 10.1109/ODICON50556.2021.9428967.
[19] T. Mohamed, H. Abubakr, M. Hussein, and G. Shabib, "Load Frequency Controller Based on Particle Swarm Optimization for Isolated Microgird System," *Int. J. Appl. Energy Syst.*, vol. 1, no. 2, pp. 69–75, 2019, doi: 10.21608/ijaes.2019.169953.
[20] M. Shouran and A. M. Alsseid, "Cascade of Fractional Order PID based PSO Algorithm for LFC in Two-Area Power System," in *Proc. ICERA 2021 3rd Int. Conf. Electron. Represent. Algorithm*, Yogyakarta, Indonesia, Jul. 29–30, 2021, pp. 1–6, doi: 10.1109/ICERA53111.2021.9538646.
[21] G. Chen, Z. Li, Z. Zhang, and S. Li, "An Improved ACO Algorithm Optimized Fuzzy PID Controller for Load Frequency Control in Multi Area Interconnected Power Systems," *IEEE Access*, vol. 8, pp. 6429–6447, 2020, doi: 10.1109/ACCESS.2019.2960380.
[22] Y. Arya, "A new optimized fuzzy FOPI-FOPD controller for automatic generation control of electric power systems," *J. Franklin Inst.*, vol. 356, no. 11, pp. 5611–5629, 2019, doi: 10.1016/j.jfranklin.2019.02.034.
[23] Y. Arya, "Improvement in automatic generation control of two-area electric power systems via a new fuzzy aided optimal PIDN-FOI controller," *ISA Trans.*, vol. 80, pp. 475–490, Sept. 2018, doi: 10.1016/j.isatra.2018.07.028.
[24] Y. Arya, "A novel CFFOPI-FOPID controller for AGC performance enhancement of single and multi-area electric power systems," *ISA Trans.*, vol. 100, pp. 126–135, 2020, doi: 10.1016/j.isatra.2019.11.025.
[25] T. Weldcherkos, A. O. Salau, and A. Ashagrie, "Modeling and design of an automatic generation control for hydropower plants using Neuro-Fuzzy controller," *Energy Reports*, vol. 7, pp. 6626–6637, 2021, doi: 10.1016/j.egyr.2021.09.143.
[26] J. H. Lanker, R. Bhushan, and N. Gupta, "Load Frequency Control of Multi Area Power System Using Meta-heuristic/Artificial Intelligence Techniques," in *Proc. 2022 Int. Conf. Intell. Controll. Comput. Smart Power, ICICCSP 2022*, Hyderabad, India, Jul. 21–23, 2022, doi: 10.1109/ICICCSP53532.2022.9862473.
[27] S. Prakash and S. K. Sinha, "Four area load frequency control of interconnected hydro-thermal power system by intelligent PID control technique," in *Proc. 2012 Students Conf. Eng. Syst. SCES 2012*, Allahabad, India, Mar. 16–18, 2012, pp. 1–6, doi: 10.1109/SCES.2012.6199090.
[28] M. I. Mosaad and F. Salem, "LFC based adaptive PID controller using ANN and ANFIS techniques," *J. Electr. Syst. Inf. Technol.*, vol. 1, no. 3, pp. 212–222, 2014, doi: 10.1016/j.jesit.2014.12.004.
[29] Y. Ma, Z. Hu, and Y. Song, "A Reinforcement Learning Based Coordinated but Differentiated Load Frequency Control Method With Heterogeneous Frequency Regulation Resources," *IEEE Trans. Power Syst.*, vol. 39, pp. 2239–2250, 2023, doi: 10.1109/TPWRS.2023.3262543.
[30] Z. Yan and Y. Xu, "Data-driven load frequency control for stochastic power systems: A deep reinforcement learning method with continuous action search," *IEEE Trans. Power Syst.*, vol. 34, no. 2, pp. 1653–1656, 2019, doi: 10.1109/TPWRS.2018.2881359.
[31] Z. Yan and Y. Xu, "A Multi-Agent Deep Reinforcement Learning Method for Cooperative Load Frequency Control of a Multi-Area Power System," *IEEE Trans. Power Syst.*, vol. 35, no. 6, pp. 4599–4608, 2020, doi: 10.1109/TPWRS.2020.2999890.
[32] M. Saklani, A. Chhetri, D. K. Saini, M. Yadav, and Y. C. Gupta, "Load frequency control of two area power systems using optimised ANFIS controller," in *Proc. 5th Int. Conf. Energy, Power, Environ. Towar. Flex. Green Energy Technol. ICEPE 2023*, Shillong, India, Jun. 15–17, 2023, pp. 1–6, doi: 10.1109/ICEPE57949.2023.10201499.

[33] D. K. Ghose, K. Tanaya, A. Sahoo, and U. Kumar, "Performance Evaluation of hybrid ANFIS model for Flood Prediction," in *Proc. 8th Int. Conf. Adv. Comput. Commun. Syst. ICACCS 2022*, Coimbatore, India, Mar. 25–26, 2022, pp. 772–777, doi: 10.1109/ICACCS54159.2022.9785002.

[34] C. U. Yeom and K. C. Kwak, "A Performance Comparison of ANFIS models by Scattering Partitioning Methods," in *Proc. 2018 IEEE 9th Annu. Inf. Technol. Electron. Mob. Commun. Conf. IEMCON 2018*, Vancouver, BC, Canada, Nov. 1–3, 2018, pp. 814–818, doi: 10.1109/IEMCON.2018.8614898.

[35] C. Srinivasa Rao, "Adaptive neuro fuzzy based load frequency control of multi area system under open market scenario," in *Proc. IEEE-International Conf. Adv. Eng. Sci. Manag. ICAESM-2012*, Nagapattinam, India, Mar. 30–31, 2012, pp. 5–10.

[36] V. Nath and D. K. Sambariya, "Design and performance analysis of adaptive neuro fuzzy controller for load frequency control of multi-power system," in *Proc. 10th Int. Conf. Intell. Syst. Control. ISCO 2016*, Coimbatore, India, Jan. 7–8, 2016, pp. 1–7, doi: 10.1109/ISCO.2016.7726986.

[37] W. Eshetu, P. Sharma, and C. Sharma, "ANFIS based load frequency control in an isolated micro grid," in *Proc. IEEE Int. Conf. Ind. Technol.*, Lyon, France, Feb. 20–22, 2018, pp. 1165–1170, doi: 10.1109/ICIT.2018.8352343.

[38] S. R. Basa Varajappa and M. S. Nagaraj, "Load frequency control of three area interconnected power system using conventional PID, fuzzy logic and ANFIS Controllers," in *Proc. 2021 2nd Int. Conf. Emerg. Technol. INCET 2021*, Belagavi, India, May 21–23, 2021, pp. 1–6, doi: 10.1109/INCET51464.2021.9456120.

[39] J. S. Jang, "ANFIS: Adaptive-Network-Based Fuzzy Inference System," *IEEE Trans. Syst. Man, Cybern. Part B Cybern.*, vol. 23, no. 3, pp. 665–685, 1993.

[40] J. S. R. Jang and C. T. Sun, "Neuro-Fuzzy Modeling and Control," *Proc. IEEE*, vol. 83, no. 3, pp. 378–406, 1995, doi: 10.1109/5.364486.

[41] M. N. M. Salleh, N. Talpur, and K. Hussain, "Adaptive neuro-fuzzy inference system: Overview, strengths, limitations, and solutions," *Lect. Notes Comput. Sci.*, vol. 10387 LNCS, pp. 527–535, Aug. 2017, doi: 10.1007/978-3-319-61845-6_52.

[42] S. A. Saadat, S. M. Ghamari, H. Mollaee, and F. Khavari, "Adaptive neuro-fuzzy inference systems (ANFIS) controller design on single-phase full-bridge inverter with a cascade fractional-order PID voltage controller," *IET Power Electron.*, vol. 14, no. 11, pp. 1960–1972, 2021, doi: 10.1049/pel2.12162.

[43] Y. O. M. Sekyere, F. B. Effah, and P. Y. Okyere, "An Enhanced Particle Swarm Optimization Algorithm via Adaptive Dynamic Inertia Weight and Acceleration Coefficients," *J. Electron. Electr. Eng.*, vol. 3, no. 1, pp. 50–64, Jan. 2024, doi: 10.37256/jeee.3120243868.

[44] D. Guha, P. K. Roy, and S. Banerjee, "A maiden application of modified grey Wolf algorithm optimized cascade tilt-integral-derivative controller in load frequency control," in *Proc. 2018 20th Natl. Power Syst. Conf. NPSC 2018*, Tiruchirappalli, India, Dec. 14–16, 2018, pp. 1–6, doi: 10.1109/NPSC.2018.8771738.

[45] Y. Arya, P. Dahiya, E. Çelik, G. Sharma, H. Gözde, and I. Nasiruddin, "AGC performance amelioration in multi-area interconnected thermal and thermal-hydro-gas power systems using a novel controller," *Eng. Sci. Technol. Int. J.*, vol. 24, no. 2, pp. 384–396, 2021, doi: 10.1016/j.jestch.2020.08.015.

[46] Y. Arya, P. Dahiya, E. Çelik, G. Sharma, H. Gözde, and I. Nasiruddin, "Engineering Science and Technology, an International Journal AGC performance amelioration in multi-area interconnected thermal and thermal-hydro-gas power systems using a novel controller," *Eng. Sci. Technol. Int. J.*, vol. 24, no. 2, pp. 384–396, 2021, doi: 10.1016/j.jestch.2020.08.015.

[47] I. K. Otchere, D. O. Ampofo, and E. A. Frimpong, "Adaptive discrete wavelet transform based technique for load frequency control," in *Proc.—2017 IEEE PES-IAS PowerAfrica Conf.*, Accra, Ghana, Jun. 27–30, 2017, pp. 589–594, doi: 10.1109/PowerAfrica.2017.7991292.

[48] S. S. Mohamed, S. H. Elbanna, and A. M. Abdel-Ghany, "Fuzzy Self-tuning Fractional Order PID Controller Design in Load Frequency Control of Power Systems," in *Proc. 2020 12th Int. Conf. Electr. Eng. ICEENG 2020*, Cairo, Egypt, Jul. 7–9, 2020, pp. 89–96, 2020, doi: 10.1109/ICEENG45378.2020.9171759.

[49] A. J. Mohammed, S. D. Al-Majidi, M. K. Al-Nussairi, M. F. Abbod, and H. S. Al-Raweshidy, "Design of a Load Frequency Controller based on Artificial Neural Network for Single-Area Power System," in *Proc. 2022 57th Int. Univ. Power Eng. Conf. Big Data Smart Grids, UPEC 2022—Proc.*, Istanbul, Turkey, Aug. 30–Sept. 2, 2022, doi: 10.1109/UPEC55022.2022.9917853.